

Mapping brain mechanical property maturation from childhood to adulthood

Grace McIlvain^a, Julie M Schneider^b, Melanie A Matyi^c, Matthew DJ McGarry^d, Zhenghan Qi^e, Jeffrey M Spielberg^c, Curtis L Johnson^{a,c,*}

^a Department of Biomedical Engineering, University of Delaware, Newark, DE, United States

^b Department of Communication Sciences and Disorders, Louisiana State University, Baton Rouge, LA, United States

^c Department of Psychological and Brain Sciences, University of Delaware, Newark, DE, United States

^d Thayer School of Engineering, Dartmouth College, Hanover, NH, United States

^e Department of Communication Sciences and Disorders, Northeastern University, Boston, MA, United States

ARTICLE INFO

Keywords:

Elastography
Viscoelasticity
Development
Cortex
Stiffness
Damping ratio

ABSTRACT

Magnetic resonance elastography (MRE) is a phase contrast MRI technique which uses external palpation to create maps of brain mechanical properties noninvasively and *in vivo*. These mechanical properties are sensitive to tissue microstructure and reflect tissue integrity. MRE has been used extensively to study aging and neurodegeneration, and to assess individual cognitive differences in adults, but little is known about mechanical properties of the pediatric brain. Here we use high-resolution MRE imaging in participants of ages ranging from childhood to adulthood to understand brain mechanical properties across brain maturation. We find that brain mechanical properties differ considerably between childhood and adulthood, and that neuroanatomical subregions have differing maturational trajectories. Overall, we observe lower brain stiffness and greater brain damping ratio with increasing age from 5 to 35 years. Gray and white matter change differently during maturation, with larger changes occurring in gray matter for both stiffness and damping ratio. We also found that subregions of cortical and subcortical gray matter change differently, with the caudate and thalamus changing the most with age in both stiffness and damping ratio, while cortical subregions have different relationships with age, even between neighboring regions. Understanding how brain mechanical properties mature using high-resolution MRE will allow for a deeper understanding of the neural substrates supporting brain function at this age and can inform future studies of atypical maturation.

1. Introduction

The human brain reaches ninety percent of adult volume by age six (Iwasaki et al., 1997; Lenroot and Giedd 2006), but it continues to undergo considerable architectural changes up into the third decade of life (Paus 2005). These structural tissue adaptations include changes in neuron density, synaptic connectivity, and glial cell distribution (Garcia et al., 2018; Budday et al., 2015), and they correspond to increasing maturity of function (Tyler 2012). These effects at the microscale are reflected on the macroscale by differences in regional brain volumes, cortical folding, and tissue vasculature (Budday and Kuhl 2020; Stiles and Jernigan 2010). Understanding how neural tissue structure changes across development is critical towards our understanding of normal brain function and development. Brain tissue mechanical properties are a sensitive metric by which underlying microstructural integrity is quantified (Hiscox et al., 2016; Johnson and Telzer 2018).

The ability to measure brain mechanical properties non-invasively is relatively new, and changes to tissue mechanical properties due to maturation have not been comprehensively studied.

Tissue mechanical properties can be measured *in vivo* using a phase contrast MRI technique called magnetic resonance elastography (MRE) (Manduca et al., 2001). MRE non-invasively captures the shear wave motion in tissue that can be used to calculate the viscoelastic shear modulus, which can be reported as shear stiffness, a measure of tissue composition, and damping ratio, a measure thought to reflect tissue organization (Sack et al., 2013). One of the most prevalent findings from MRE is that the brain decreases in mechanical integrity during normal healthy aging (Sack et al., 2011; Arani et al., 2015; Hiscox et al., 2018). It has been shown that the magnitude of these changes is comparable to, or greater than, the declines found using other quantitative imaging measures, highlighting an increased sensitivity of MRE to detect subtle neural changes (Davis et al., 2009; Kennedy et al.,

* Corresponding author: Department of Biomedical Engineering, University of Delaware 150 Academy St, Newark, DE 19716, United States.
E-mail address: clj@udel.edu (C.L. Johnson).

2009; Lebel et al., 2012). Brain mechanical integrity is particularly susceptible to neurodegenerative disorders including Alzheimer's disease (Murphy et al., 2011; 2016; Hiscox et al., 2020), Parkinson's disease (Lipp et al., 2013; 2018), and multiple sclerosis (Wuerfel et al., 2010; Streitberger et al., 2012). Recent advancements in MRE imaging and image processing technology now allow brain MRE measures to be analyzed on a regional basis (Johnson et al., 2016; Daugherty et al., 2020), which has helped to provide more specific insights into aging and disease (Hiscox et al. 2021). Interestingly, these regional brain MRE measures have proved sensitive enough to even reflect differences in cognitive performance (Schwarb et al., 2016) and have been shown to be more sensitive to cognitive function than other larger-scale structural changes such as volume (Schwarb et al., 2017).

While MRE is growing in popularity and scope for understanding neurodegeneration and cognitive function, brain mechanical changes during neurodevelopment have only been studied for the first time recently and in a very limited fashion (McIlvain et al., 2018; Yeung et al., 2019; Ozkaya et al., 2021; McIlvain et al., 2020; Chaze et al. 2019). Brain maturation is characterized by several neurobiological signatures that are expected to impact mechanical integrity. Between childhood and adulthood, neural tissue remodeling occurs through synaptic pruning, a process which results in volumetric changes and alterations in the underlying tissue microstructure (Paolicelli et al., 2011); however, it is challenging to thoroughly study these structural changes *in vivo* without advanced neuroimaging techniques. Notably, different regions of the brain experience synaptic pruning and other structural maturation phenomena at different rates. Lower order functions develop first, and higher order functions have a much longer period of maturation, with the prefrontal cortex being one of the last regions to reach full maturity (Kolk and Rakic 2022). Quantifying differential time courses of structural maturation across these regions will complement our existing understanding of the associations between regional brain maturation and maturation of related functions and provide an overall sensitive window into brain health during this time period.

Here we aim to report how the brain matures in mechanical properties on a regional basis using a fast, high-resolution MRE sequence in participants aged 5–35 years. We examine the relationships with age for global brain mechanical properties as well as individual subcortical and cortical gray matter structures. We aim to identify how brain mechanical properties mature regionally, and to understand how regions exhibit different relationships with age. Characterizing brain tissue microstructural integrity in the pediatric population is a vital step towards a comprehensive understanding of key structure function relationships, and towards informing future studies of neurodevelopmental disorders.

2. Methods

A total of 125 subjects ages 5–35 years old (63 Males, 62 Females) were recruited from the community surrounding the University of Delaware. These subjects participated in one of several ongoing imaging studies, each of which had an identical MRE and anatomical MRI protocol. All subjects were healthy, neurotypical, and right-handed. Age distribution can be found in *Supplemental Information Figure S1*. All studies were approved by the University of Delaware Institutional Review Board and all participants, and guardians of the minor participants, gave informed written consent.

2.1. Image acquisition

Each participant completed a scan session on a Siemens 3T Prisma MRI scanner with a 64-channel head coil (Siemens Medical Solutions; Erlangen, Germany). The imaging session included a high-resolution, T_1 -weighted MPRAGE sequence (magnetization-prepared rapidly-acquired gradient echo; $0.9 \times 0.9 \times 0.9 \text{ mm}^3$; TR/TI/TE=2300/900/2.32 ms) for anatomical localization and an MRE acquisition.

The MRE experiment uses externally generated mechanical vibrations to create micron level displacements of brain tissue. These brain displacements can be captured through motion-encoding MRI sequences under different encoding conditions including axis of motion encoding, polarity of motion encoding, and in time via varying synchronization to achieve a series of phase offsets. Here we used a 3D multiband, multishot spiral MRE sequence (Johnson et al., 2016) to achieve high spatial resolution, with OSCILLATE (McIlvain et al., 2022) to reduce scanning time through sparse sampling and low-rank image reconstruction, making it ideally suited for scanning a pediatric population. The MRE sequence encoded displacements at 50 Hz from vibrations delivered to the head with a pneumatic actuator system and soft pillow driver (Resoundant; Rochester, MN). k -space sampling trajectories were designed to have 4 k_z -planes and 4 in plane k_{xy} -shots. Data was collected with SENSE parallel imaging (Pruessmann et al., 2001) undersampling both in-plane and through-plane ($R_{xy}=2$ and $R_z=2$) and was additionally spatiotemporally undersampled in an alternating k_{xy} shot pattern for each of the 24 repetitions for an additional OSCILLATE reduction factor of $R_{OSC}=2$, which was on top of the undersampling from SENSE. Other imaging parameters included: $240 \times 240 \text{ mm}^2$ FOV; 160×160 matrix; $1.5 \times 1.5 \times 1.5 \text{ mm}^3$ resolution; bilateral, flow-compensated, matched-period motion-encoding gradients at 70 mT/m; and 4 evenly-spaced phase offsets. For subjects aged 5–10 a smaller z-field of view of 64 slices was used (TR/TE = 2240/70 ms; acquisition time 3 min 35 s), and for older subjects aged 11–35, 80 slices were collected (TR/TE = 2800/76 ms; acquisition time 4 min 28 s). These age ranges were conservatively chosen to ensure whole brain MRE images for all participants, while minimizing the scan time for the youngest subjects with the smallest heads. Additionally, a separately collected B_0 field mapping scan was acquired with the same number of slices as image data and parameters including: $240 \times 240 \text{ mm}^2$ FOV; 160×160 matrix; and TR/TE₁/TE₂ = 800/15.0/15.6 ms. MRE data was reconstructed using an iterative low-rank reconstruction technique in PowerGrid (Cerjanic et al., 2016), which uses graphical processing units (GPUs) to enable faster image reconstruction. The reconstruction leverages parallel imaging by using a phase-corrected SENSE algorithm that includes correction for B_0 field inhomogeneities (Sutton et al., 2003) and motion induced phase errors (Johnson et al., 2014; Liu et al., 2004). All images were visually inspected for motion errors prior to inclusion in the data set; images corrupted by subject motion were excluded.

2.2. Image processing and analysis

MRE displacement fields were determined from the reconstructed phase images. FMRIB Software Library (FSL) PRELUDE (Jenkinson 2003) was used to unwrap MRE data and temporal Fourier filtering returned complex harmonic displacement fields (Manduca et al., 2001). A nonlinear inversion algorithm (NLI) (McGarry et al., 2012) was used to calculate maps of viscoelastic shear stiffness and damping ratio from the MRE displacement fields. NLI returns whole brain mechanical property maps of the complex viscoelastic shear modulus ($G^* = G' + iG''$), with G' as the storage modulus and G'' as the loss modulus. The viscoelastic shear stiffness, μ , can be calculated as $\mu = 2|G|^2 / (G' + |G|)$ (Manduca et al., 2001) and damping ratio, ξ , can be calculated as $\xi = G'' / 2G'$ (McGarry and Van Houten, 2008). In NLI, soft prior regularization (SPR) (McGarry et al., 2013) incorporates *a priori* spatial information to improve the measures of cortical and subcortical gray matter regions. This involves providing masks of each neuroanatomical region over which property variation is penalized during parameter optimization (Johnson et al., 2016; Schwarb et al., 2016), which has the effect of reducing influences from surrounding tissue and improving regional measures.

To generate regions-of-interest (ROIs) the T_1 -weighted anatomical image was segmented in FreeSurfer (FS) v 6.0.0 (Dale et al., 1999). Global brain regions included the subcortical gray matter, cortical gray matter, cortical white matter, and the whole cerebrum which was a com-

bination of all regions. We also examined individual subcortical and cortical regions. Subcortical gray matter regions included the amygdala, hippocampus, caudate, pallidum, putamen, thalamus. Cortical regions included the frontal, parietal, occipital, temporal, and cingulate lobes, as well as some notable subcomponents of interest within these lobes. The subcomponents of the frontal lobe included the inferior frontal gyrus (IFG), the orbital frontal cortex (OFC), the dorsolateral prefrontal cortex (dlPFC), the ventromedial prefrontal cortex (vmPFC), and the motor cortex. Parietal lobe subcomponents included the superior parietal lobe, inferior parietal lobe, and somatosensory cortex. Temporal lobe subcomponents included the superior temporal lobe, the middle temporal lobe, and the inferior temporal lobe. Cerebrospinal fluid (CSF) was also segmented from the MPRAGE using FSL FAST (Zhang et al., 2001). Any voxel with greater than 10% CSF was excluded from analysis, as fluid is not modeled by the MRE inversion and CSF can affect property outcomes (Murphy et al., 2013). All regions were registered to MRE space using a linear affine transformation with 6-degrees of freedom in FSL FLIRT (Jenkinson et al., 2002), and used as individual regions for SPR during NLI. Regional mechanical property maps were created by multiplying each ROI mask with the maps of mechanical properties, and the regions were spatially averaged to obtain one resulting value. FreeSurfer was also used to obtain the volumes of each global and subcortical gray matter region and the thickness of each cortical gray matter region.

2.3. Statistical analysis

Analyses were performed using IBM SPSS Statistics for Mac, version 28.0.1.1 (IBM Corp., Armonk, NY, USA). A repeated measured analysis of variance (ANOVA) was used to test whether mechanical properties varied with region, with age, and differently with age between regions (region \times age interaction effect). Separate models were used for stiffness and damping ratio in each of the three major categories of ROIs: whole brain, subcortical structures, and cortical structures. Tukey *post hoc* tests were used to identify age relationships for each region, and pairwise comparisons between structures were calculated based on the estimated marginal means, with Bonferroni adjustments made for multiple comparisons. Stiffness and damping ratio were linearly regressed against age separately for each ROI and correlation coefficients, r , were calculated for each relationship of regional measure with age. Steiger's Z test (Steiger 1980) was used to compare relationships with age between regions, the complete results of which can be found in *Supplemental Information Tables S1-S6*. An analysis of mechanical property relationships between structures was conducted by running a partial correlation with age between each pair of structures. Sex differences in brain mechanical property maturation were considered by using ANOVA to test whether the age \times sex interaction was significant for each ROI, with Bonferroni correction for multiple comparisons. A paired *t*-test was used to compare the mechanical properties of each structure between the left and right brain hemisphere for each ROI, with Bonferroni correction. A comparison of the volume and the mechanical properties of each structure was conducted using a Pearson's correlation, controlling for age, with Bonferroni correction. Finally, the line of best fit of each property vs. age for each region was evaluated at ages 5 and 35 years, and percent differences between these time points were calculated as the difference relative to age 5, with annual rate of change calculated as difference between age 5 and 35 divided by 30 years.

3. Results

Fig. 1 illustrates how brain stiffness and damping ratio change with maturation. Using an omnibus ANOVA test, we found in people ages 5–35 that brain stiffness is significantly lower with advancing age ($F = 21.77$; $p < 0.001$), while brain damping ratio is significantly greater with advancing age ($F = 14.46$; $p < 0.001$). Fig. 2 shows that the stiffness of the cerebrum is significantly correlated with age ($r = -0.37$; p

< 0.001) and appears to decrease from an average stiffness of 3.17 kPa at age 5 to an average stiffness of 2.87 kPa at age 35, which is approximately a 9.4% reduction in stiffness. Mechanical properties of each global tissue subtype – white matter, cortical gray matter, and subcortical gray matter – also change significantly with age ($p < 0.01$). It is seen in Table 1 that between ages 5 and 35 white matter, on average, appears to decrease just 0.006 kPa per year, or approximately 5.2%, which is less change than the average cerebrum (z-score: -5.61 ; $p < 0.001$). Conversely cortical gray matter appears to decrease 14.4% from 5 to 35, which is a stronger age effect than the overall cerebrum (z-score: 4.06; $p < 0.001$). Cortical and subcortical gray matter have considerably different magnitudes at all time points during development – 3.20 kPa and 4.37 kPa respectively at age 5, and 2.74 kPa and 3.47 kPa respectively at age 35 (pairwise *post hoc* test significance of $p < 0.001$) – but do not exhibit significant differences in the rate of change with age (z-score: -0.86 ; $p = 0.389$).

We observed significant increases in cerebral damping ratio with age of 14.7% from age 5 to 35 ($p < 0.001$). Similar to stiffness, damping ratio of cortical gray matter has the strongest age effect of the global regions. Gray matter changes at an approximate rate of 0.9% per year ($r = 0.68$; $p < 0.001$) or a total change of 27.3% between ages 5 and 35, which is slightly greater than the average cerebrum at an approximate rate of 0.5% per year ($r = 0.61$; $p < 0.001$), and significantly greater (z-score: 4.59; $p < 0.001$) than the white matter rate of change of 0.27% per year ($r = 0.33$; $p < 0.001$).

We additionally examined age related effects on subcortical gray matter structures. From the omnibus ANOVA test, we found that at the group level there were significant age-related differences in both the stiffness ($F = 6.36$; $p < 0.001$) and damping ratio ($F = 4.24$; $p = 0.001$). Fig. 3 presents the relationships of stiffness of each subcortical structure with age, where all the subcortical structures exhibit significantly lower stiffness with advancing age ($r = -0.24$ to -0.56 ; $p < 0.05$), except for the amygdala ($r = -0.05$; $p = 0.57$). However, for damping ratio, only the hippocampus ($r = 0.25$; $p = 0.005$), caudate ($r = 0.29$; $p = 0.001$), and thalamus ($r = 0.29$; $p = 0.001$) show significant age-related changes, with each structure exhibiting greater damping ratio with age. Table 1 shows that the caudate and thalamus have the largest magnitude of change in both mechanical property measures between 5 and 35: stiffness decreases of 1.45 kPa and 0.98 kPa, respectively (33.2% and 22.7%), and damping ratio increases 0.058 and 0.042, respectively (26.5% and 22.2%). The pallidum and putamen are related structures which exhibit similar age relationships for both stiffness – 0.51 kPa and 0.61 kPa decreases from 5 to 35 respectively; both $p < 0.01$ (z-score: 1.68; $p = 0.092$) – and non-significant age effects in damping ratio. The amygdala and hippocampus are both medial temporal lobe structures and have similar damping ratio age effects between them (z-score: -0.78 ; $p = 0.44$), however, only the hippocampus significantly increases with age ($r = 0.25$; $p = 0.005$). The hippocampus also significantly decreases in stiffness with age ($r = -0.25$; $p = 0.004$), while the relationship of amygdala stiffness with age is not significant, and these two relationships are significantly different (z-score: -2.54 ; $p < 0.001$).

We see in Figs. 4 and 5 that the stiffness of the cortical gray matter also shows overall significant effects with age ($F = 10.53$; $p < 0.001$), and differential patterns of maturation between lobes, even between subregions of the same lobe. Cortical stiffness significantly decreases with age between 5 and 35, with changes occurring to the major lobar regions at a variable rate between 11.6% in the occipital cortex ($r = -0.32$; $p < 0.001$) to 24.9% in the cingulate cortex ($r = -0.62$; $p < 0.001$; Table 2). Interestingly, even the subregions of a single lobe showed differing patterns of maturation. For example, in the frontal cortex, stiffness of the OFC and IFG mature very similarly (z-score: -0.44 ; $p = 0.661$), each changing less than 12% between the ages of 5 and 35, which is the smallest of nearly any cortical changes. And the dlPFC and vmPFC have similar slopes of decline in stiffness 20.5% and 17.8% respectively (z-score -0.81 ; $p = 0.418$), but the vmPFC is considerably stiffer at all ages (*post hoc* pairwise comparisons, $p < 0.001$).

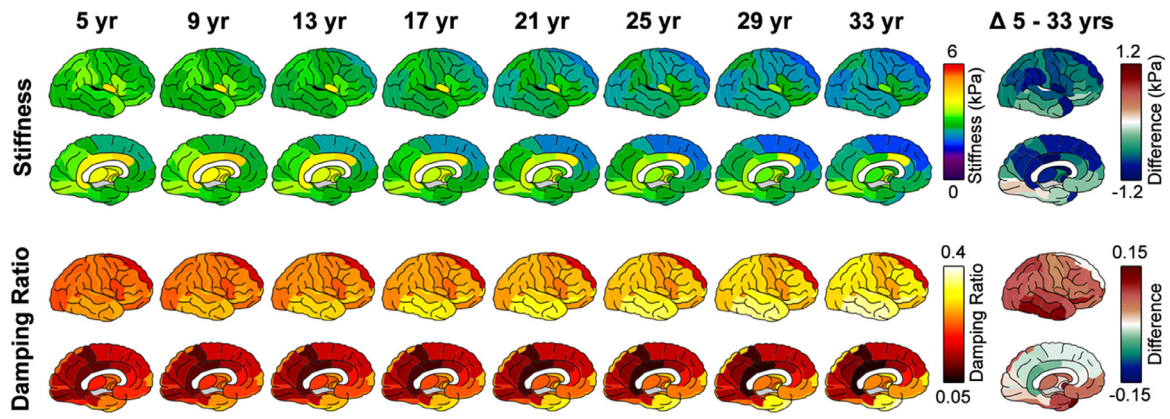


Fig. 1. Brain stiffness and damping ratio at eight time points during maturation, as well as differences in mechanical properties between age 5 and age 35. Changes in blue represent decreases in mechanical properties with age, while red represents increases. (For interpretation of the references to color in this figure legend, the reader is referred to the web version of this article.)

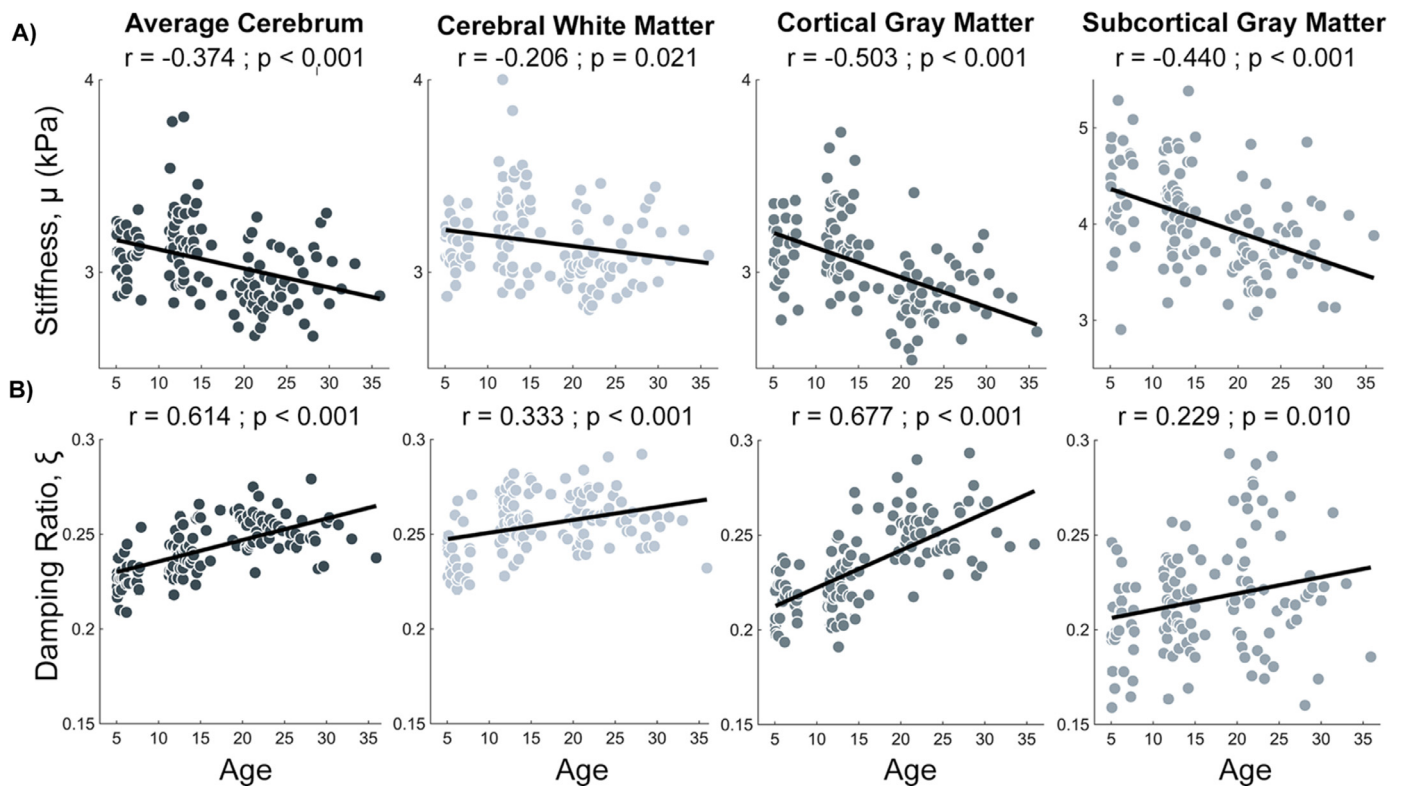


Fig. 2. Brain mechanical property maturation from ages 5 to 35 for the cerebrum, white matter, cortical gray matter, and subcortical gray matter for A) shear stiffness, μ , and B) damping ratio, ξ , measured using MRE.

Table 1

Stiffness and damping ratio of global brain regions and subcortical gray matter structures evaluated at ages 5 and 35 years old, and apparent annual differences in properties for regions with significant relationships with age (* indicating $p < 0.05$).

Structure	Stiffness (kPa)			Damping Ratio				
	Age 5	Age 35	Δ /yr	Age 5	Age 35	Δ /yr		
Cerebrum	3.167	2.871	-0.010	*	0.230	0.264	0.001	*
White Matter	3.220	3.052	-0.006	*	0.247	0.268	0.001	*
Cortical GM	3.204	2.741	-0.015	*	0.213	0.271	0.002	*
Subcortical GM	4.365	3.466	-0.030	*	0.206	0.232	0.001	*
Amygdala	3.689	3.583	N.S.		0.212	0.242	N.S.	
Hippocampus	3.105	2.595	-0.017	*	0.195	0.232	0.001	*
Pallidum	4.207	3.694	-0.017	*	0.226	0.224	N.S.	
Putamen	4.479	3.869	-0.020	*	0.218	0.212	N.S.	
Caudate	4.364	2.915	-0.048	*	0.220	0.278	0.002	*
Thalamus	4.324	3.342	-0.033	*	0.190	0.232	0.001	*

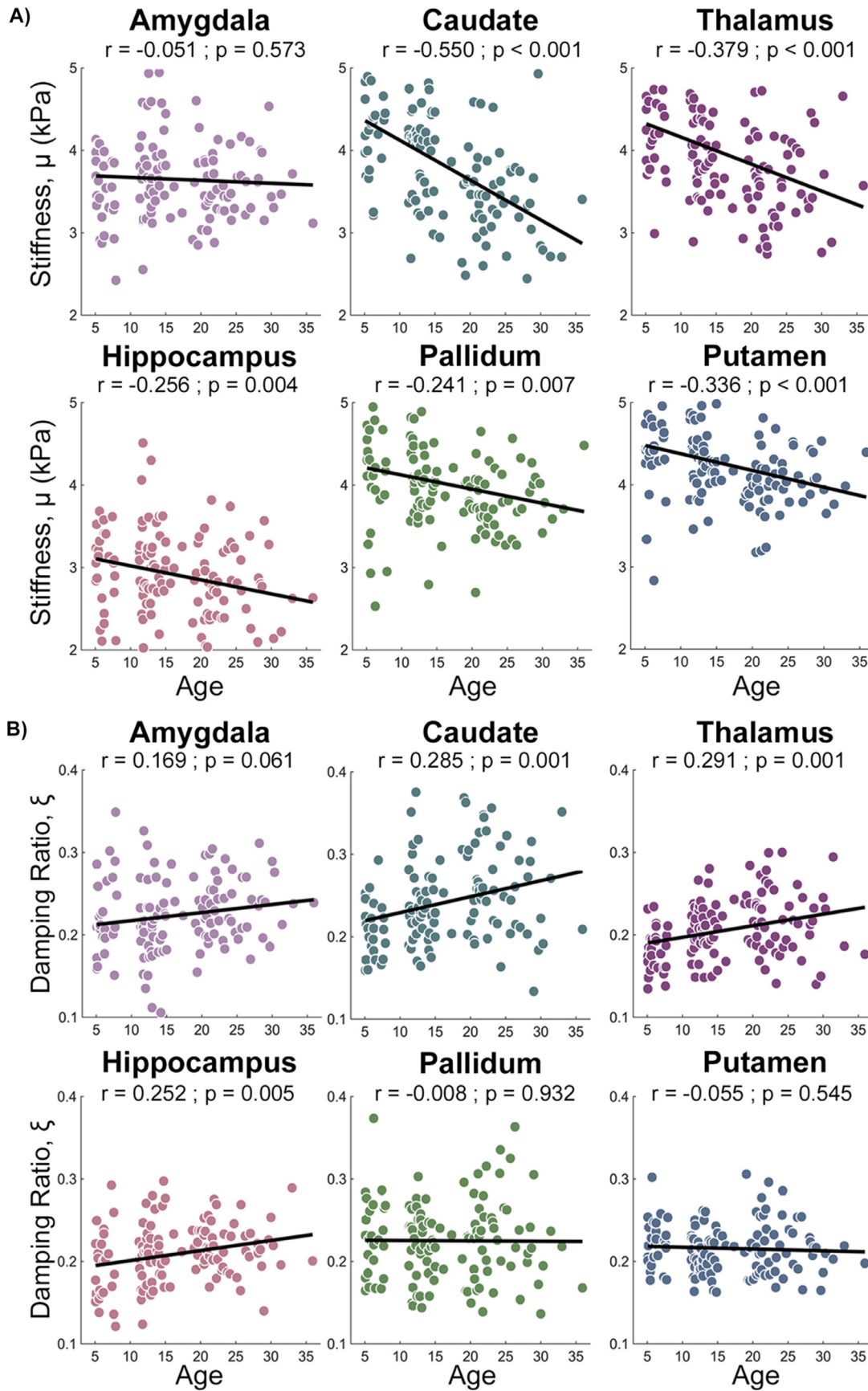


Fig. 3. Mechanical properties of the subcortical structures amygdala, hippocampus, caudate, pallidum, putamen, and thalamus during maturation from ages 5–35 years old for A) shear stiffness, μ , and B) damping ratio, ξ , measured using MRE.

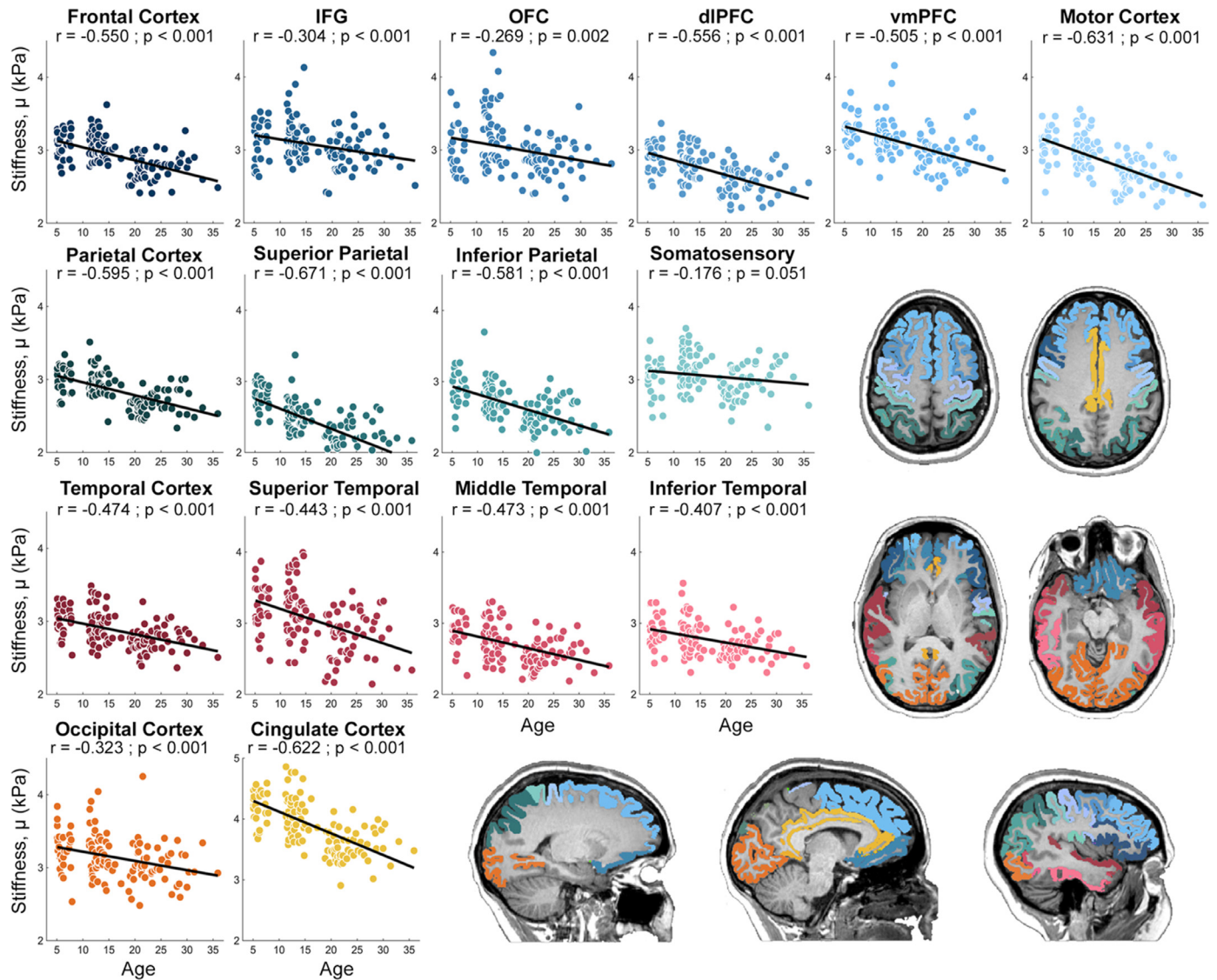


Fig. 4. Mechanical property maturation of cortical shear stiffness μ of the frontal, parietal, temporal, occipital and cingulate lobes and their subcomponents from ages 5–35 years old.

Table 2

Stiffness and damping ratio of cortical gray matter structures evaluated at ages 5 and 35 years old. An ANOVA was used to determine significance of correlations with age, which are demarcated with a * for $p < 0.05$.

Structure	Stiffness (kPa)			Damping Ratio				
	Age 5	Age 35	Δ /yr	Age 5	Age 35	Δ /yr		
Avg. Frontal	3.129	2.592	-0.018	*	0.197	0.233	0.001	*
IFG	3.202	2.864	-0.011	*	0.247	0.303	0.001	*
OFC	3.169	2.794	-0.013	*	0.203	0.281	0.003	*
dlPFC	2.961	2.352	-0.021	*	0.185	0.164	-0.001	*
vmPFC	3.322	2.730	-0.020	*	0.204	0.228	0.001	*
Motor Cortex	3.156	2.393	-0.025	*	0.214	0.263	0.002	*
Avg. Parietal	3.050	2.517	-0.018	*	0.215	0.258	0.001	*
Superior	2.754	1.915	-0.028	*	0.219	0.304	0.003	*
Inferior	2.931	2.275	-0.022	*	0.230	0.308	0.003	*
Somatosensory	3.123	2.942	-0.006		0.228	0.264	0.001	*
Avg. Temporal	3.041	2.604	-0.015	*	0.236	0.327	0.003	*
Superior	3.321	2.604	-0.024	*	0.242	0.329	0.003	*
Middle	2.895	2.402	-0.016	*	0.262	0.359	0.003	*
Inferior	2.917	2.537	-0.013	*	0.259	0.379	0.004	*
Avg. Occipital	3.283	2.902	-0.013	*	0.171	0.224	0.002	*
Avg. Cingulate	4.299	3.229	-0.036	*	0.113	0.084	-0.001	*

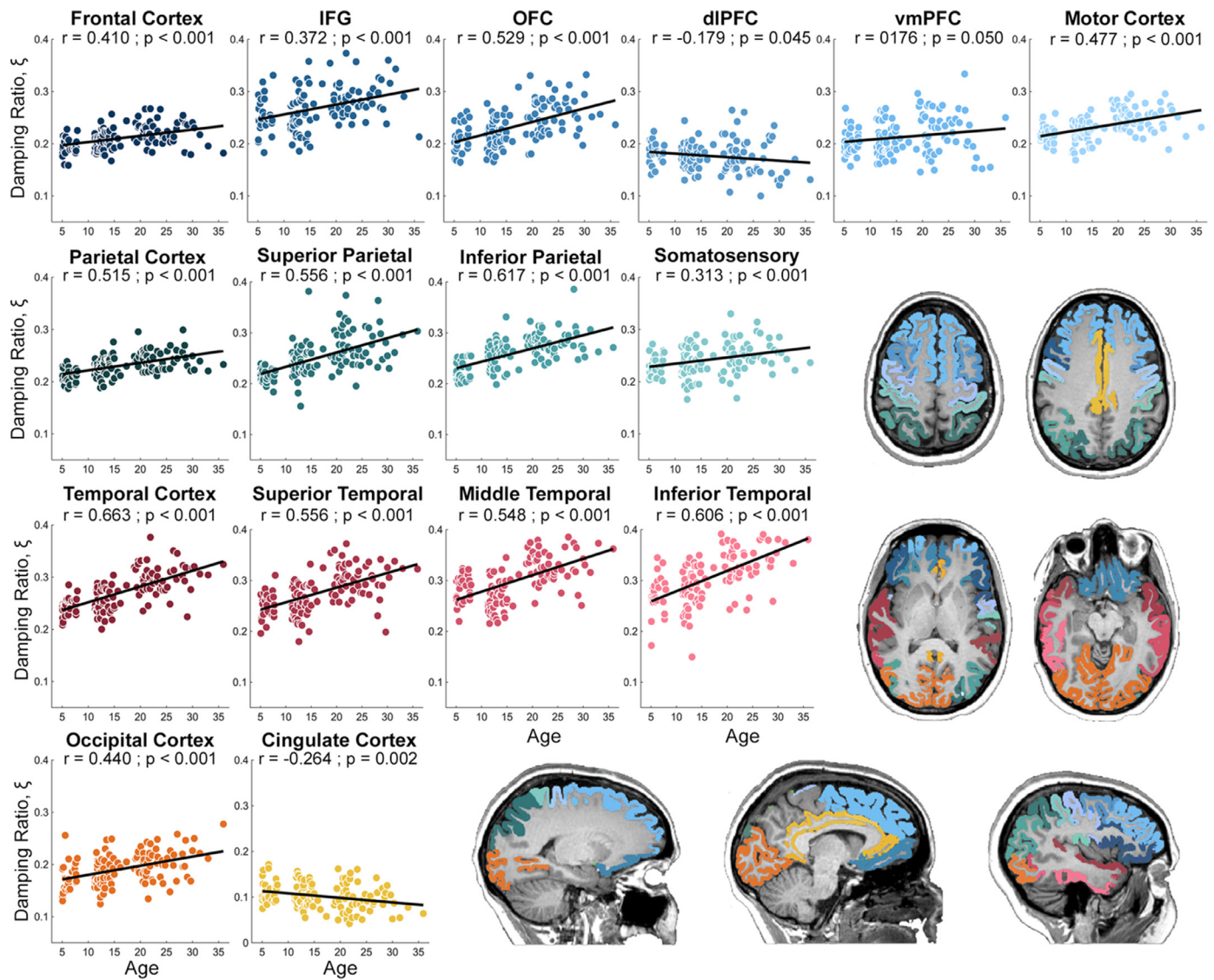


Fig. 5. Mechanical property maturation of cortical damping ratio of the frontal, parietal, temporal, occipital and cingulate lobes and their subcomponents from ages 5–35 years old.

The subcomponents of the parietal lobe decrease in stiffness at different rates, with the inferior parietal cortex being only 0.177 kPa stiffer than the superior parietal cortex at age 5, but 0.360 kPa stiffer by age 35 (z-score -1.97 ; $p = 0.048$). Most different of all is stiffness of the somatosensory cortex, which does not significantly differ with age ($r = -0.18$; $p = 0.051$) and thus has different age effects compared to superior and inferior parietal lobes (z-scores of 5.76 and 4.58; both $p < 0.001$). Most interestingly, the motor cortex and the somatosensory cortex, which are anatomically adjacent regions, are vastly different in their developmental trajectories, with a z-score of -6.89 ($p < 0.001$). Finally, the cingulate cortex, which is the only of the major cortex regions located interior to the brain, has a distinctly different pattern of development. At all ages it is stiffer than the other cortical regions (*post hoc* pairwise comparisons with all cortical regions $p < 0.001$), and it has the largest rate of stiffness change of any of region (changing 1.069 kPa, or 24.9% between 5 and 35 years), indicating that the cingulate cortex is the least similar to other regions in 5-year-olds and becomes more similar during maturation.

Table 2 illustrates that all cortical gray matter regions change significantly in damping ratio with age ($p < 0.001$), however the rate of change of structures vary significantly between many regions. Damping ratio

shows the highest cortical rates of change in the temporal and occipital cortex with a 38.2% and 30.6% increase between ages 5 and 35, respectively (Fig. 5). In contrast, the frontal cortex and parietal cortex change less drastically at 18.2% and 20.1% and show no significant differences in rate of change between them (z-score: -1.51 ; p-value = 0.132). The cingulate is the only of the average lobar regions that decreases in damping ratio with age and has a significantly different slope than every other major lobar region (*post hoc* pairwise comparisons with all cortical regions $p < 0.01$), with a 26.2% decrease between ages 5 and 35. In the subregions of the frontal lobe the IFG (23.0%, $r = 0.37$; $p < 0.001$), OFC (38.3%, $r = 0.53$; $p < 0.001$) and vmPFC (12.1%, $r = 0.18$; $p = 0.050$) all significantly increase with age, whereas the dlPFC decreases in damping ratio with age at 11.1% between ages 5 and 35 ($r = -0.18$; $p = 0.045$). In contrast to stiffness, the motor cortex and the somatosensory cortex do not have significantly different maturational trajectories in damping ratio (z-score: 1.95; $p = 0.051$). It can be seen in Fig. 1 that lateral brain regions appear to increase in damping ratio with age, while medial regions appear to decrease in damping ratio with age. Broadly, damping ratio appears to get less similar between structures as age increases, which is in contrast to stiffness, which generally becomes more similar with advancing age.

We found that regions were often correlated with one other in stiffness, such that the relative stiffness of any given region is likely to describe the relative stiffness of the other regions. This same finding was however not true for damping ratio, where individual differences in each structure are expected to be significant. These results are consistent with a previous similar study on a small group of young adults (Johnson et al., 2016). The complete pairwise analysis can be found in *Supplemental Information Tables S7 and S8*. We also found that stiffness and volume were in general not correlated with each other. Only damping ratio of the vmPFC ($r = -0.28$; $p = 0.001$), superior parietal lobe ($r = -0.28$, $p = 0.001$), and inferior parietal lobe ($p = -0.28$; $p = 0.001$) were significantly correlated with volume after correction for multiple comparisons. Some correlation between MRE properties and volume is expected as they both will vary with age, but the general lack of significant relationships is expected given previous studies that have shown independence in these parameters and that MRE outcomes are not significantly biased by volume (Schwarb et al., 2016; Hiscox et al., 2022; Scott et al., 2022; Hiscox et al., 2020). Full results are found in *Supplemental Information Table S9*. Interestingly, there were no significant age \times sex interaction effects in any region or property; complete results can be found in *Supplemental Information Figures S2-S5*.

We also found notable hemispheric differences in pediatric brain mechanical properties. Of the whole brain and subcortical structure regions, all were stiffer in the right hemisphere, and all were significantly different after correction for multiple comparisons, except for the amygdala, hippocampus, and thalamus. The cerebrum was on average 2.90% more stiff in the right hemisphere at age 5 ($p < 0.001$). The caudate showed the largest hemispheric differences, at age 5 being 5.19% more stiff on the right, and at age 35 being 10.90% stiffer on the right ($p < 0.001$). The cortical regions were all stiffer in the right hemisphere at age 5, except for the cingulate cortex, but by age 35, the left and right hemisphere were very similar in stiffness. Damping ratio was, in general, higher in the left hemisphere at age 5, but showed only a few consistent significant hemispheric differences when considering the entire age range. Complete hemispheric results are presented in *Supplemental Information Table S10 and S11*.

4. Discussion

Using fast, high-resolution MR elastography, we characterized brain mechanical property maturation in participants aged 5–35 years and found regionally different relationships between stiffness and damping ratio with age. We found that, on average, the global cerebrum appears to decrease in stiffness with maturation while appearing to increase in damping ratio. Notably, cortical and subcortical gray matter exhibit strong age effects in both stiffness and damping ratio, whereas white matter shows only weak age effects. Of the subcortical structures, we found that the caudate and thalamus appear to change the most with age in both stiffness and damping ratio. Cortical regions exhibit different age effects between lobes, but also even cortical subregions within a single lobe appear to change differently.

It has been well established that cerebral stiffness decreases during normal aging and that this decrease is accelerated in people with neurodegenerative disease (Hiscox et al., 2021). The brain has been estimated to decrease in stiffness at a rate of about 0.3% per year in younger and middle aged adults (Takamura et al., 2020) and a rate of approximately 0.4% per year in older adults (Sack et al., 2009). Comparatively, here we find a whole cerebrum stiffness decrease of approximately 0.3% per year from age 5 to age 35 (relative to age 5 stiffness). Prior to this work, it was unknown how brain properties change across maturation, as there are only three previous pediatric MRE studies examining age effects (Yeung et al., 2019; Ozkaya et al., 2021; McIlvain et al., 2018). Compared to these prior works, our study is the first to observe changes in the average stiffness of the cerebrum across maturation. However, these prior studies were likely less sensitive to age effects given the high degree of individual variability in me-

chanical properties as they each used fewer subjects or narrower study design: 26 subjects age 7–17 (Ozkaya et al., 2021), 47 subjects age 7–44 (Yeung et al., 2019), and children in the narrow age range of just 12–14 compared with male adults aged 18–33 (McIlvain et al., 2018). Here we assess 125 subjects distributed in age from 5 to 35 years, making this study more suited to observing age-related differences. Also, only one of these previous pediatric publications has reported regional brain properties, and found, despite a lack of whole brain findings, that several regional brain substructures significantly differed between adolescents and adults (McIlvain et al., 2018). There are some regional discrepancies in the direction of mechanical property maturation compared to our current work, but the previous focused solely on groups of adolescents compared to adults, which could mask larger trends across the age range, or may point to potential nonlinear trends in brain mechanical properties with age, particularly around the period of adolescence.

Here we investigated age related variations to subcortical and cortical gray matter structures, which show significantly different relationships between mechanical properties with age during the period of brain maturation. For example, at age five, the caudate, thalamus, pallidum, and putamen have relatively similar average stiffness, but by age 35, the caudate and thalamus have decreased in stiffness more than twice as much as the pallidum and putamen, and the amygdala does not change significantly with age at all. Stiffness relationships with age in the subcortical gray matter regions agree with our previous work which also reported decreases in mechanical properties of the caudate and the putamen between adolescence and adulthood and showed similar trends in stiffness of the medial temporal lobe (McIlvain et al., 2018). In children and adolescents, a progressive loss of volume has been found in the basal ganglia regions, with increases in volume of the medial temporal lobe regions, which supports that there exists differential patterns of maturation in these structural groups (Toga et al., 2006). We believe that the maturational trends of mechanical properties in these structures reflect evolving brain microstructure which could relate to how associated functions mature. Here we showed that while both volume and mechanical properties change with age, they are generally not correlated with each other, indicating that these independent measures both require consideration in understanding brain structural maturation.

In the cerebral cortex, we found that even regions within the same lobe had notably different mechanical property values and relationships with age. The cortex is of paramount interest in neurodevelopment as it changes dramatically in the first three decades of life and controls many basic brain functions including vision, hearing, speech, planning, and emotional control (Toga et al., 2006; Levitt 2003). Cortical maturation had not previously been investigated using MRE, with only a few studies reporting cortical mechanical property in the adult brain. However, using high-resolution MRE imaging (Hiscox et al., 2022), here we are able to identify several cortical mechanical property developmental trends. Of note is the difference in stiffness maturation between the adjacent regions of the motor cortex and the somatosensory cortex. These two cortical regions are known to be some of the first to begin to develop (Gogtay et al., 2004; Jay et al. 1999), but it is expected that lower-order structures such as the somatosensory cortex will be among the first brain regions to fully develop (Gogtay et al., 2004; Hammelrath et al., 2016), and this developmental completion might occur before the youngest age analyzed in this study.

While the biological basis of the mechanical properties measured with MRE is not completely known, there are several microstructural phenomena which are hypothesized to be linked to mechanical property measures. In healthy young adults, stiffness is understood to be a measure of tissue composition (Johnson and Telzer 2018), including neuron density and myelin concentration (Freimann et al., 2013; Schregel et al., 2012), whereas damping ratio is thought to be a measure of tissue organization (Sack et al., 2013). In development, a major aspect of neural architectural remodeling is the process of synaptic pruning, resulting in substantial thinning of the cerebral cortex; simultaneously, individual neurons are forming more axon terminals, resulting in increases in vol-

ume of white matter (Giedd et al., 2012; Jay et al. 1999). Here we see that mechanical properties change more in gray matter with maturation, which may be a result of the synaptic pruning process, though more pre-clinical work is required to understand these changes. Interestingly, a recent MRE animal study showed a maturation-driven increase in stiffness in regions including the hippocampus and thalamus, and a stiffness decrease in a number of cortical regions including the somatosensory and motor cortex regions (Guo et al., 2019). While the findings in the murine subcortical regions contradict the findings we see here, this is not necessarily unexpected due to fundamental differences in structure and development of murine and human brains. Most interestingly, this murine study also demonstrated that specific structural protein up- and down-regulation during development are reflected through mechanical property measurements and, specifically, that proteins related to cell adhesion more often changed concurrently with tissue stiffness while structural plasticity changed concurrently with damping ratio (Guo et al., 2019). Finally, we see here that there may be notable hemispheric differences, particularly at the younger age group of our analysis, which is consistent with previous cognitive theories that brain hemispheres develop asymmetrically (Toga and Thompson 2003). Understanding the biological mechanisms of mechanical property change is critical towards a robust understanding of brain health and development during maturation.

Stiffness has been the primary measure of brain tissue integrity reported using MRE, with damping ratio only recently becoming of interest owing to the development of methods capable of reliably estimating this property (Solamen et al., 2018), and the observation of notable relationships with cognitive function. In adults, the brain has been shown to increase in damping ratio with age and neurodegeneration, unexpectedly here we also find an apparent increase to both global and regional damping ratio in the developing brain (Lv et al., 2020; Delgorio et al. 2021). Interestingly the lateral and medial regions of the brain follow different damping ratio developmental trajectories, with lateral regions appearing to increase in damping ratio during development while medial regions appear to decrease during development. It remains unclear what direction of change constitutes as beneficial changes in damping ratio within this age range, or what the biological underpinnings of changes to damping ratio are. In most adult MRE studies, including normal aging, higher stiffness and lower damping ratio have been considered to reflect improved brain structural integrity (Schwarb et al., 2017; Johnson et al. 2018; Schwarb et al., 2016; Daugherty et al., 2020; Schwarb et al., 2019; Hiscox et al., 2018). Our results, however, indicate that through the course of brain maturation the brain is softer and has higher damping ratio, thus we cannot assume that our interpretation of better or worse brain mechanical properties is necessarily valid in pediatric populations. Several pediatric studies of functional performance have found agreement with adult literature that higher stiffness is associated with better performance (McIlvain et al., 2020, et al. 2020; Schneider et al., 2022) and that atypical development was associated with lower brain stiffness (Chaze et al. 2019), however in each of these studies, age was within a very limited range or was included as a regressed coefficient. The existence of these studies reveals the plausibility that in pediatrics, for individuals at the same age or developmental stage, higher stiffness and lower damping still reflect better functional performance, while across maturation the age effect is opposite. Further we expect that atypical development will still result in reduced brain stiffness, indicative of damage to neural tissue. More pediatric brain MRE studies are necessary to determine the dual role of aging and cognitive performance in measured brain stiffness and damping ratio.

The major limitation of this study is that it was cross-sectional. While the age relationships reported here reflect expected trends of mechanical property maturation, there is a pressing need for longitudinal studies in the pediatric brain (King et al. 2018; Mills et al., 2014). Longitudinal measures provide a way to parse age-related brain changes separate from individual differences in the population, which is critical towards establishing mechanical properties as correlates of functional perfor-

mance and other aspects of brain development and to more completely understand sex differences in brain maturation (Becht and Mills, 2020; Jay N. Giedd et al., 1999; Mills and Tamnes, 2014). Additionally, longitudinal maturational trajectories can be modeled as nonlinear with age. Nonlinearity in brain mechanical property development is expected as brain development is controlled by a number of biological processes which up and down regulate on different time courses in different areas of the brain (Norbom et al., 2021). Furthermore, many neuroimaging modalities, including most commonly in diffusion (Lebel et al., 2008, 2017) and volumetry (Gogtay et al., 2004; Ball et al., 2012), demonstrate nonlinearity of brain development and emphasize regional dependencies. A contributing factor to the nonlinear development of brain mechanical properties are changes which occur during puberty. It is well established that adolescence is a time of immense remodeling to neuronal structure. While this study was not designed to capture the effects of sex or puberty on brain mechanical properties, close examination of our data suggests that at approximately age 15 there may be a sudden decrease in brain stiffness in some regions. Animal models have shown a similarly sharp reduction in the number of neurons and number of synaptic connections available immediately following puberty, particularly in females (Juraska and Drzewiecki 2020). Further, we had a limited sample size at the oldest ages of inclusion, making accurately modeling sex differences across the entire age range more challenging. Finally, the biological underpinnings of changes to brain mechanical properties during maturation are not thoroughly understood. More work in human brain and in animal models are needed to understand the dynamic changes between age, function, and mechanical properties throughout brain maturation. A robust understanding about how the brain changes from longitudinal measures, and how these measures relate to functional performance, are particularly necessary to provide a foundation of typical development for investigating cases of atypical neurodevelopment.

5. Conclusion

Our study provides the first comprehensive examination of *in vivo* brain mechanical properties during maturation in people ages 5–35 years and uses high-resolution imaging and advanced MRE methods to allow for reliable regional mechanical property estimates. The results of this work indicate that brain stiffness significantly differs with age both globally and regionally during maturation from childhood to adulthood, and these changes fit well within the context of time courses of regional brain development. Identifying MRE as a sensitive metric for measuring maturational changes to brain tissue presents future opportunities to identify how maturation of function is reflected by maturation of brain mechanical properties, and to use brain mechanics as a metric of improvement in cognitive interventions. Understanding brain mechanical property development is critical to gain deeper insights to structure function relationships during development and to inform future studies investigating the neural basis of neurodevelopmental disorders.

Ethical statement

This research was conducted in accordance with *The Code of Ethics of the World Medical Association*. This study was approved by the University of Delaware Institutional Review Board and all participants, and guardians of the minor participants, gave informed written consent prior to being studied.

Data availability statement

Numerical data will be made available by simple request. Raw image files will be made available by request which includes a formal project outline and an agreement of data sharing.

Conflict of Interest

There are no known conflicts of interest associated with this publication and there has been no significant financial support for this work that could have influenced its outcome.

Credit authorship contribution statement

Grace McIlvain: Conceptualization, Data curation, Formal analysis, Methodology, Writing – original draft. **Julie M Schneider:** Data curation, Funding acquisition, Writing – review & editing. **Melanie A Matyi:** Data curation, Writing – review & editing. **Matthew DJ McGarry:** Methodology, Resources, Software, Writing – review & editing. **Zhenghan Qi:** Funding acquisition, Writing – review & editing. **Jeffrey M Spielberg:** Funding acquisition, Writing – review & editing. **Curtis L Johnson:** Methodology, Resources, Supervision, Validation, Funding acquisition, Writing – review & editing.

Acknowledgments

This work was supported in part by NIH grants [R01-EB027577](#), [U01-NS112120](#), [R01-AG058853](#), [F31-HD103361](#), [R01-MH123470](#), [P20-GM103653](#) (Delaware Neuroscience COBRE), and [P20-GM103446](#) (Delaware INBRE), and NSF grant [SBE SPRF-FR 1911462](#).

Supplementary materials

Supplementary material associated with this article can be found, in the online version, at doi:[10.1016/j.neuroimage.2022.119590](#).

References

- Arani, A., Murphy, M.C., Glaser, K.J., Manduca, A., Lake, D.S., Kruse, S.A., Jack, C.R., Ehman, R.L., Huston, J., 2015. Measuring the effects of aging and sex on regional brain stiffness with MR elastography in healthy older adults. *Neuroimage* 111, 59–64. doi:[10.1016/j.neuroimage.2015.02.016](#).
- Ball, W.S., Byars, A.W., Schapiro, M., Bommer, W., Carr, A., German, A., Dunn, S., et al., 2012. Total and regional brain volumes in a population-based normative sample from 4 to 18 years: the NIH MRI study of normal brain development. *Cereb. Cortex* 22 (1), 1–12. doi:[10.1093/cercor/bhr018](#).
- Becht, A.L., Mills, K.L., 2020. Modeling individual differences in brain development. *Biol. Psychiatry* 88 (1), 63–69. doi:[10.1016/j.biopsych.2020.01.027](#).
- Budday, S., Kuhl, E., 2020. Modeling the life cycle of the human brain. *Curr. Opin. Biomed. Eng.* 15, 16–25. doi:[10.1016/j.cobme.2019.12.009](#).
- Budday, S., Steinmann, P., Kuhl, E., 2015. Physical biology of human brain development. *Front. Cell. Neurosci.* 9, 1–17. doi:[10.3389/fncel.2015.00257](#), JULY.
- Cerjanic, A., Holtrop, J.L., Ngo, G.C., Leback, B., Arnold, G., Moer, M.V., LaBelle, G., Fessler, J.A., Sutton, B.P., 2016. PowerGrid: a open source library for accelerated iterative magnetic resonance image reconstruction. *Proc. Intl. Soc. Mag. Reson. Med. Reson. Abstract #0525*.
- Dale, A.M., Fischl, B., Sereno, M.I., 1999. Cortical surface-based analysis. *Neuroimage* 9 (2), 179–194. doi:[10.1006/nimg.1998.0395](#).
- Daugherty, A.M., Schwarb, H.D., McGarry, M.D.J., Johnson, C.L., Cohen, N.J., 2020. Magnetic resonance elastography of human hippocampal subfields: ca3-dentate gyrus viscoelasticity predicts relational memory accuracy. *J. Cogn. Neurosci.* 32 (9), 1704–1713. doi:[10.1162/jocn_a.01574](#).
- Davis, S.W., Dennis, N.A., Buchler, N.G., White, L.E., Madden, D.J., Cabeza, R., 2009. Assessing the effects of age on long white matter tracts using diffusion tensor tractography. *Neuroimage* 46 (2), 530–541. doi:[10.1016/j.neuroimage.2009.01.068](#).
- Delgado, Peyton, L., Hiscox, L.V., Daugherty, A.M., Sanjana, F., Pohlig, R.T., Ellison, J.M., Martens, C.R., Schwarb, H., McGarry, M.D.J., Johnson, C.L., 2021. Effect of aging on the viscoelastic properties of hippocampal subfields assessed with high-resolution MR elastography. *Cerebr. Cortex* 31 (6), 2799–2811. doi:[10.1093/cercor/bhaa388](#).
- Freimann, F.B., Mueller, S., Streitberger, K.-J., Guo, J., Rot, S., Ghorri, A., Vajkoczy, P., et al., 2013. MR elastography in a murine stroke model reveals correlation of macroscopic viscoelastic properties of the brain with neuronal density. *NMR Biomed.* 26, 1534–1539. doi:[10.1002/nbm.2987](#).
- Garcia, K.E., Kroenke, C.D., Bayly, P.V., 2018. Mechanics of cortical folding: stress, growth and stability. *Philos. Trans. R. Soc. B: Biol. Sci.* 373. doi:[10.1098/rstb.2017.0321](#), 1759.
- Giedd, J.N., Blumenthal, J., Jeffries, N.O., Castellanos, F.X., Lin, H., Zijdenbos, A., Paus, T., Evans, A.C., Rapoport, J.L., 1999a. Brain development during childhood and adolescence: a longitudinal MRI study. *Nat. Neurosci.* 10 (2), 861–863. [http://neurosci.nature.com](#).
- Giedd, J.N., Raznahan, A., Mills, K.L., Lenroot, R.K., 2012. Review: magnetic resonance imaging of male/female differences in human adolescent brain anatomy. *Biol. Sex Differ.* 3 (1), 1–9. doi:[10.1186/2042-6410-3-19](#).
- Gogtay, N., Giedd, J.N., Lusk, L., Hayashi, K.M., Greenstein, D., Vaituzis, A.C., Nugent, T.F., et al., 2004. Dynamic mapping of human cortical development during childhood through early adulthood. *Proc. Natl. Acad. Sci. USA* 101 (21), 8174–8179. doi:[10.1073/pnas.0402680101](#).
- Guo, J., Bertalan, G., Meierhofer, D., Klein, C., Schreyer, S., Steiner, B., Wang, S., et al., 2019. Brain maturation is associated with increasing tissue stiffness and decreasing tissue fluidity. *Acta Biomater.* 99, 433–442. doi:[10.1016/j.actbio.2019.08.036](#).
- Hammelrath, L., Škokić, S., Khmelinskii, A., Hess, A., Knaap, N.V.D., Staring, M., Lelieveldt, B.P.F., Wiedermann, D., Hoehn, M., 2016. Morphological maturation of the mouse brain: an in vivo MRI and histology investigation. *Neuroimage* 125, 144–152. doi:[10.1016/j.neuroimage.2015.10.009](#).
- Hiscox, L., Johnson, C.L., McGarry, M.D.J., Perrins, M., Littlejohn, A., Beek, E.J.R.V., Roberts, N., Starr, J.M., 2018a. High-resolution magnetic resonance elastography reveals differences in subcortical gray matter viscoelasticity between young and healthy older adults. *Neurobiol. Aging* 65, 158–167. doi:[10.1016/j.neurobiolaging.2018.01.010](#).
- Hiscox, L., Johnson, C.L., McGarry, M.D.J., Schwarb, H., R Van Beek, E.J., Roberts, N., Starr, J.M., 2018b. Hippocampal viscoelasticity and episodic memory performance in healthy older adults examined with magnetic resonance elastography. *Brain Imaging Behav.* doi:[10.1007/s11682-018-9988-8](#).
- Hiscox, L.V., McGarry, M.D.J., Johnson, C.L., 2022. Evaluation of cerebral cortex viscoelastic property estimation with nonlinear inversion magnetic resonance elastography. *Phys. Med. Biol.* 67 (9), 095002.
- Hiscox, L.V., Johnson, C.L., Barnhill, E., McGarry, M.D.J., Huston, J., Beek, E.J.R.V., Starr, J.M., Roberts, N., 2016. Magnetic resonance elastography (MRE) of the human brain: technique, findings and clinical applications. *Phys. Med. Biol.* 61, R401–R437. doi:[10.1088/0031-9155/61/24/R401](#).
- Hiscox, L.V., Johnson, C.L., McGarry, M.D.J., Marshall, H., Ritchie, C.W., Beek, E.J.R.V., Roberts, N., Starr, J.M., 2020. Mechanical property alterations across the cerebral cortex due to alzheimer's disease. *Brain Commun.* 2 (1), 1–16. doi:[10.1093/brain-comms/fcz049](#).
- Hiscox, Lucy, V., Schwarb, H., McGarry, M.D.J., Johnson, C.L., 2021. Aging brain mechanics: progress and promise of magnetic resonance elastography. *Neuroimage* 232, 117889. doi:[10.1016/j.neuroimage.2021.117889](#).
- Iwasaki, N., Hamano, K., Okada, Y., Horigome, Y., Nakayama, J., Takeya, T., Takita, H., Nose, T., 1997. Volumetric quantification of brain development using MRI. *Neuroradiology* 39 (12), 841–846. doi:[10.1007/s002340050517](#).
- Jenkinson, M., 2003. Fast, automated, n-dimensional phase-unwrapping algorithm. *Magn. Reson. Med.* 49 (1), 193–197. doi:[10.1002/mrm.10354](#).
- Jenkinson, M., Bannister, P., Brady, M., Smith, S., 2002. Improved optimization for the robust and accurate linear registration and motion correction of brain images. *Neuroimage* 17 (2), 825–841. doi:[10.1016/S1053-8119\(02\)91132-8](#).
- Johnson, C.L., Holtrop, J.L., McGarry, M.D.J., Weaver, J.B., Paulsen, K.D., Georgiadis, J.G., Sutton, B.P., 2014. 3D multislabs, multishot acquisition for fast, whole-brain MR elastography with high signal-to-noise efficiency. *Magn. Reson. Med.* 71 (2), 477–485. doi:[10.1002/mrm.25065](#).
- Johnson, Curtis, L., Schwarb, H., Horecka, K.M., Matthew, D.J., McGarry, J., Hillman, C.H., Kramer, A.F., Cohen, N.J., Barbey, A.K., 2018. Double dissociation of structure-function relationships in memory and fluid intelligence observed with magnetic resonance elastography. *Neuroimage* 171, 99–106. doi:[10.1016/j.neuroimage.2018.01.007](#), December 2017.
- Johnson, C.L., Schwarb, H., McGarry, M.D.J., Anderson, A.T., Huesmann, G.R., Sutton, B.P., Cohen, N.J., 2016a. Viscoelasticity of subcortical gray matter structures. *Hum. Brain Mapp.* 37, 4221–4233. doi:[10.1002/hbm.23314](#).
- Johnson, C.L., Telzer, E.H., 2018. Magnetic resonance elastography for examining developmental changes in the mechanical properties of the brain. *Dev. Cogn. Neurosci.* 33, 176–181. doi:[10.1016/j.dcn.2017.08.010](#).
- Johnson, C.L., Holtrop, J.L., Anderson, A.T., Sutton, B.P., 2016b. Brain MR elastography with multiband excitation and nonlinear motion-induced phase error correction. In: *24th Annual Meeting of the International Society for Magnetic Resonance in Medicine, Singapore*, p. 1951.
- Juraska, J.M., Drzewiecki, C.M., 2020. Cortical reorganization during adolescence: what the rat can tell us about the cellular basis. *Dev. Cogn. Neurosci.* 45, 100857. doi:[10.1016/j.dcn.2020.100857](#).
- Kennedy, K.M., Erickson, K.I., Rodrigue, K.M., Voss, M.W., Colcombe, S.J., Kramer, A.F., Acker, J.D., Raz, N., 2009. Age-related differences in regional brain volumes: a comparison of optimized voxel-based morphometry to manual volumetry. *Neurobiol. Aging* 30 (10), 1657–1676. doi:[10.1016/j.neurobiolaging.2007.12.020](#).
- King, Kevin, M., Littlefield, A.K., McCabe, C.J., Mills, K.L., John Flournoy, and Laurie Chassin, 2018. Longitudinal modeling in developmental neuroimaging research: common challenges, and solutions from developmental psychology. *Dev. Cogn. Neurosci.* 33, 54–72. doi:[10.1016/j.dcn.2017.11.009](#), February 2017.
- Kolk, S.M., Rakic, P., 2022. Development of prefrontal cortex. *Neuropsychopharmacology* 47 (1), 41–57. doi:[10.1038/s41386-021-01137-9](#).
- Lebel, C., Gee, M., Camicioli, R., Wielar, M., Martin, W., Beaulieu, C., 2012. Diffusion tensor imaging of white matter tract evolution over the lifespan. *Neuroimage* 60 (1), 340–352. doi:[10.1016/j.neuroimage.2011.11.094](#).
- Lebel, C., Walker, L., Leemans, A., Phillips, L., Beaulieu, C., 2008. Microstructural maturation of the human brain from childhood to adulthood. *Neuroimage* 40 (3), 1044–1055. doi:[10.1016/j.neuroimage.2007.12.053](#).
- Lebel, C., Treit, S., Beaulieu, C., 2017. A review of diffusion MRI of typical white matter development from early childhood to young adulthood. *NMR Biomed.* 32 (4), 1–23. doi:[10.1002/nbm.3778](#).
- Lenroot, R.K., Giedd, J.N., 2006. Brain development in children and adolescents: insights from anatomical magnetic resonance imaging. *Neurosci. Biobehav. Rev.* 30 (6), 718–729. doi:[10.1016/j.neubiorev.2006.06.001](#).

- Levitt, P., 2003. Structural and functional maturation of the developing primate brain. *J. Pediatr.* 143 (4 SUPPL), 35–45. doi:10.1067/s0022-3476(03)00400-1.
- Lipp, A., Skowronek, C., Fehlner, A., Streitberger, K.-J., Braun, J., Sack, I., 2018. Progressive supranuclear palsy and idiopathic Parkinson's disease are associated with local reduction of in vivo brain viscoelasticity. *Eur. Radiol.* 28 (8), 3347–3354. doi:10.1007/s00330-017-5269-y.
- Lipp, A., Trbojevic, R., Paul, F., Fehlner, A., Hirsch, S., Scheel, M., Noack, C., Braun, J., Sack, I., 2013. Cerebral magnetic resonance elastography in supranuclear palsy and idiopathic Parkinson's disease. *NeuroImage: Clin.* 3, 381–387. doi:10.1016/j.nicl.2013.09.006.
- Liu, C., Bammer, R., Kim, D.H., Moseley, M.E., 2004. Self-navigated interleaved spiral (SNAILS): application to high-resolution diffusion tensor imaging. *Magn. Reson. Med.* 52 (6), 1388–1396. doi:10.1002/mrm.20288.
- Lv, H., Kurt, M., Zeng, N., Ozkaya, E., Marcuz, F., Wu, L., Laksari, K., et al., 2020. MR elastography frequency-dependent and independent parameters demonstrate accelerated decrease of brain stiffness in elder subjects. *Eur. Radiol.* 30 (12), 6614–6623. doi:10.1007/s00330-020-07054-7.
- Manduca, A., Oliphant, T.E., Alex Dresner, M., Mahowald, J.L., Kruse, S.A., Amromin, E., Felmlee, J.P., Greenleaf, J.F., Ehman, R.L., 2001. Magnetic resonance elastography: non-invasive mapping of tissue elasticity. *Med. Image Anal.* 5 (4), 237–254. doi:10.1016/S1361-8415(00)00039-6.
- McGarry, M.D.J., Houten, E.E.W.V., Johnson, C.L., Georgiadis, J.G., Sutton, B.P., Weaver, J.B., Paulsen, K.D., 2012. Multiresolution MR elastography using nonlinear inversion. *Med. Phys.* 39 (10), 6388–6396. doi:10.1118/1.4754649.
- McGarry, M.D.J., Houten, E.E.W.V., 2008. Use of a Rayleigh damping model in elastography. *Med. Biol. Eng. Comput.* 46 (8), 759–766. doi:10.1007/s11517-008-0356-5.
- McGarry, M., Johnson, C.L., Sutton, B.P., Houten, E.E.V., Georgiadis, J.G., Weaver, J.B., Paulsen, K.D., 2013. Including spatial information in nonlinear inversion MR elastography using soft prior regularization. *IEEE Trans. Med. Imaging* 32 (10), 1901–1909. doi:10.1109/TMI.2013.2268978.
- McIlvain, G., Cerjanic, A.M., McGarry, M.D.J., Christodoulou, A.G., Johnson, C.L., 2022. OSCILLATE: a low-rank approach for accelerated magnetic resonance elastography. *Magn. Reson. Med.* 88, 1659–1672.
- McIlvain, G., Clements, R.G., Magoon, E.M., Spielberg, J.M., Telzer, E.H., Johnson, C.L., 2020a. Viscoelasticity of reward and control systems in adolescent risk taking. *Neuroimage* 215, 116850. doi:10.1016/j.neuroimage.2020.116850.
- McIlvain, G., Schwarb, H., Cohen, N.J., Telzer, E.H., Johnson, C.L., 2018. Mechanical properties of the in vivo adolescent human brain. *Dev. Cogn. Neurosci.* 34, 27–33. doi:10.1016/j.dcn.2018.06.001.
- McIlvain, G., Tracy, J.B., Chaze, C.A., Petersen, D., Wright, H., Miller, F., Crenshaw, J.R., Johnson, C.L., 2020b. Brain stiffness relates to dynamic balance reactions in children with cerebral palsy. *J. Child Neurol.* 35 (7), 463–471. doi:10.1177/0883073820909274.
- Mills, K.L., Tamnes, C.K., 2014. Methods and considerations for longitudinal structural brain imaging analysis across development. *Dev. Cogn. Neurosci.* 9, 172–190. doi:10.1016/j.dcn.2014.04.004.
- Mills, K.L., Goddings, A.-I., Clasen, L.S., Giedd, J.N., Blakemore, S.J., 2014. The developmental mismatch in structural brain maturation during adolescence. *Dev. Neurosci.* 36, 147–160. doi:10.1159/000362328.
- Murphy, M.C., Huston, J., Jack, C.R., Glaser, K.J., Manduca, A., Felmlee, J.P., Ehman, R.L., 2011. Decreased brain stiffness in Alzheimer's disease determined by magnetic resonance elastography. *J. Magn. Reson. Imaging* 34 (3), 494–498. doi:10.1002/jmri.22707.
- Murphy, M.C., Huston, J., Jack, C.R., Glaser, K.J., Senjem, M.L., Chen, J., Manduca, A., Felmlee, J.P., Ehman, R.L., 2013. Measuring the characteristic topography of brain stiffness with magnetic resonance elastography. *PLoS ONE* 8 (12), e81668. doi:10.1371/journal.pone.0081668.
- Murphy, M.C., Jones, D.T., Jack, C.R., Glaser, K.J., Senjem, M.L., Manduca, A., Felmlee, J.P., Carter, R.E., Ehman, R.L., Huston, J., 2016. Regional brain stiffness changes across the Alzheimer's disease spectrum. *NeuroImage: Clin.* 10, 283–290. doi:10.1016/j.nicl.2015.12.007.
- Norbom, L.B., Ferschmann, L., Parker, N., Agartz, I., Andreassen, O.A., Paus, T., Westlye, L.T., Tamnes, C.K., 2021. New insights into the dynamic development of the cerebral cortex in childhood and adolescence: integrating macro- and microstructural MRI findings. *Prog. Neurobiol.* 204. doi:10.1016/j.pneurobio.2021.102109, June.
- Ozkaya, E., Fabris, G., Macruz, F., Suar, Z.M., Abderezaei, J., Su, B., Laksari, K., et al., 2021. Viscoelasticity of children and adolescent brains through MR elastography. *J. Mech. Behav. Biomed. Mater.* 115, 104229. doi:10.1016/j.jmbbm.2020.104229.
- Paolicelli, R.C., Bolasco, G., Pagani, F., Maggi, L., Scianni, M., Panzanelli, P., Giustetto, M., et al., 2011. Synaptic pruning by microglia is necessary for normal brain development. *Science* 333 (6048), 1456–1458. doi:10.1126/science.1202529.
- Paus, T., 2005. Mapping brain maturation and cognitive development during adolescence. *Trends Cogn. Sci. (Regul. Ed.)* 9 (2), 60–68. doi:10.1016/j.tics.2004.12.008.
- Pruessmann, K.P., Weiger, M., Börner, P., Boesiger, P., 2001. Advances in sensitivity encoding with arbitrary K-space trajectories. *Magn. Reson. Med.* 46 (4), 638–651. doi:10.1002/mrm.1241.
- Sack, I., Beierbach, B., Wuerfel, J., Klatt, D., Hamhaber, U., Papazoglou, S., Martus, P., Braun, J., 2009. The impact of aging and gender on brain viscoelasticity. *Neuroimage* 46 (3), 652–657. doi:10.1016/j.neuroimage.2009.02.040.
- Sack, I., Jöhrens, K., Würfel, J., Braun, J., 2013. Structure-sensitive elastography: on the viscoelastic powerlaw behavior of in vivo human tissue in health and disease. *Soft Matter* 9 (24), 5672–5680. doi:10.1039/c3sm50552a.
- Sack, I., Streitberger, K.J., Krefling, D., Paul, F., Braun, J., 2011. The influence of physiological aging and atrophy on brain viscoelastic properties in humans. *PLoS ONE* 6 (9), 1–7. doi:10.1371/journal.pone.0023451.
- Schneider, J.M., McIlvain, G., Johnson, C.L., 2022. Mechanical properties of the developing brain are associated with language input and vocabulary outcome. *Dev. Neuropsychol.* 47 (5), 258–277. doi:10.1080/87565641.2022.2108425.
- Schregel, K., Wuerfel, E., Garteiser, P., Gemeinhardt, I., Prozorovski, T., Aktas, O., Merz, H., Petersen, D., Wuerfel, J., Sinkus, R., 2012. Demyelination reduces brain parenchymal stiffness quantified in vivo by magnetic resonance elastography. *Proc. Natl. Acad. Sci.* 109 (17), 6650–6655. doi:10.1073/pnas.1200151109/-/DCSupplemental.www.pnas.org/cgi/doi/10.1073/pnas.1200151109.
- Schwarb, H., Johnson, C.L., Daugherty, A.M., Hillman, C.H., Kramer, A.F., Cohen, N.J., Barbey, A.K., 2017. Aerobic fitness, hippocampal viscoelasticity, and relational memory performance. *Neuroimage* 153, 179–188. doi:10.1016/j.neuroimage.2017.03.061.
- Schwarb, H., Johnson, C.L., McGarry, M.D.J., Cohen, N.J., 2016. Medial temporal lobe viscoelasticity and relational memory performance. *Neuroimage* 132, 534–541. doi:10.1016/j.neuroimage.2016.02.059.
- Schwarb, H., Johnson, C.L., Dulas, M.R., McGarry, M.D.J., Holtrop, J.L., Watson, P.D., Wang, J.X., Voss, J.L., Sutton, B., Cohen, N.J., 2019. Structural and functional MRI evidence for distinct medial temporal and prefrontal roles in context-dependent relational memory. *J. Cogn. Neurosci.* 31 (12), 1857–1872.
- Scott, Jonathan, M., Pavuluri, K.D., Trzasko, J.D., Manduca, A., Senjem, M.L., Huston, J., Ehman, R.L., Murphy, M.C., 2022. Impact of material homogeneity assumption on cortical stiffness estimates by MR elastography. *Magn. Reson. Med.* 88 (2), 916–929. doi:10.1002/mrm.29226.
- Solamen, L.M., McGarry, M.D.J., Tan, L., Weaver, J.B., 2018. Phantom evaluations of nonlinear inversion MR elastography. *Phys. Med. Biol.* 63 (14), 145021.
- Steiger, J.H., 1980. Tests for comparing elements of a correlation matrix. *Psychol. Bull.* 87, 245–251.
- Stiles, J., Jernigan, T.L., 2010. The basics of brain development. *Neuropsychol. Rev.* 20 (4), 327–348. doi:10.1007/s11065-010-9148-4.
- Streitberger, K.J., Sack, I., Krefling, D., Pfüller, C., Braun, J., Paul, F., Wuerfel, J., 2012. Brain viscoelasticity alteration in chronic progressive multiple sclerosis. *PLoS ONE* 7 (1), e29888. doi:10.1371/journal.pone.0029888.
- Sutton, B.P., Noll, D.C., Fessler, J.A., 2003. Fast, iterative image reconstruction for MRI in the presence of field inhomogeneities. *IEEE Trans. Med. Imaging* 22 (2), 178–188.
- Takamura, T., Motosugi, U., Sasaki, Y., Kakegawa, T., Sato, K., Glaser, K.J., Ehman, R.L., Onishi, H., 2020. Influence of age on global and regional brain stiffness in young and middle-aged adults. *J. Magn. Reson. Imaging* 51 (3), 727–733. doi:10.1002/jmri.26881.
- Toga, A.W., Thompson, P.M., 2003. Mapping brain asymmetry. *Nat. Rev. Neurosci.* 4 (1), 37–48. doi:10.1038/nrn1009.
- Toga, A.W., Thompson, P.M., Sowell, E.R., 2006. Mapping brain maturation. *Focus (Madison)* 4 (3), 378–390. doi:10.1176/foc.4.3.378.
- Tyler, W.J., 2012. The mechanobiology of brain function. *Nat. Rev. Neurosci.* 13 (12), 867–878. doi:10.1038/nrn3383.
- Wuerfel, J., Paul, F., Beierbach, B., Hamhaber, U., Klatt, D., Papazoglou, S., Zipp, F., Martus, P., Braun, J., Sack, I., 2010. MR-elastography reveals degradation of tissue integrity in multiple sclerosis. *Neuroimage* 49 (3), 2520–2525. doi:10.1016/j.neuroimage.2009.06.018.
- Yeung, J., Jugé, L., Hatt, A., Bilston, L.E., 2019. Paediatric brain tissue properties measured with magnetic resonance elastography. *Biomech. Model. Mechanobiol.* 18 (5), 1497–1505. doi:10.1007/s10237-019-01157-x.
- Zhang, Y., Brady, M., Smith, S., 2001. Segmentation of brain MR images through a hidden Markov random field model and the expectation-maximization algorithm. *IEEE Trans. Med. Imaging* 20 (1), 45–57. doi:10.1109/42.906424.